Cloning and functional analysis of JnCYCD3;1 in *Jatropha nigroviensrugosus*

Xiao Feng
Guizhou University
Zhao Yang (zhy737@126.com)
https://orcid.org/0000-0002-2558-9216
Wang Xiu-Rong
Guizhou University

Research article

Keywords: Jatropha nigroviensrugosus, JnCYCD3:1, female to male flower ratio, intron retention, functional verification

Posted Date: March 31st, 2020

DOI: https://doi.org/10.21203/rs.3.rs-19877/v1

Abstract

Background: As a new variety of *Jatropha*, the female to male flower ratio and yield of *Jatropha nigroviensrugosus* are higher than the common *J. curcas*. Using pre-transcriptome data, the full-length gene sequence, subcellular function localization, and verification of the transgenic function were obtained in order to understand the specific functions of differentially expressed genes (DEGs).

Results: Results revealed that the open reading frame (ORF) of *J. nigroviensrugosus CYCD3;1* (*JnCYCD3;1*) was 414 bp long, encoding 137 amino acids (aa). Compared to *J. curcas*, the presence of intron retention led to early termination of the coding frame. *JnCYCD3;1* had the highest expression in new leaves, which was 68.42 times root expression, followed by inflorescence buds. The *JnMYC2* ORF was 2025 bp, encoding 674 aa. *JnMYC2* had the highest expression levels in inflorescence buds. *JnCYCD3;1* functioned in the nucleus, while *JnMYC2* was distributed in both the nucleus and cytoplasm and may possess transmembrane membrane behavior. Bimolecular fluorescence complementation (BIFC) experiments indicated that *JnMYC2* interacted with *JnCYCD3;1*. *JnCYCD3;1* transgenic tobacco considerably advanced the reproductive cycle and may promote flower formation and transformation.

Conclusions: The related experiments obtained new *CYCD3;1* transcript, verified that *CYCD3;1* is related to flower bud differentiation, proved the interaction between hormones-related genes. The study provides a new research direction for gene function of *CYCD3;1*.

Background

Jatropha nigroviensrugosus CV Yang is a natural mutant of Jatropha curcas L that was discovered by Yang et al. [1] through field investigations. Compared to J. curcas L, J. nigroviensrugosus has more female flowers, a greater proportion of female to male flowers, and a higher seed yield [2]. Several previous studies have been conducted on how to adjust the proportion of male to female flowers and increase overall seed yield. Most studies focus on the flowering process of J. curcas [3–5], before and after hormone treatment [6–7]. However, preliminary research data are lacking on the differences between cultivars in the expression of flower buds. In a previous study, the MYC2, CYCD3, and DELLA genes were found to be up-regulated during the formation of J. nigroviensrugosus inflorescence buds, and these genes may be involved in male flower primordial abortion and the determination of female flowers [8]. In order to investigate the regulatory mechanism of transition from monoecious to gynoecious plants, a comparative transcriptome analysis between gynoecious and monoecious inflorescences was conducted. Six homologous genes, including knotted1-like homeobox gene 6 (KNAT6) and MYC2, may be candidate genes for sex differentiation [9]. During the flower bud stage in Rhododendron, transcripts of MYC2, TIR1, CYCD3, COL-1, and EIN3 peak [10]. Additionally, up-regulation of CYCD3 is thought to be associated with increased inflorescence meristems of J. curcas [11].

CYCD3;1 is an unstable protein (half-life, 7 min) that is involved in cell cycle regulation. As a plant hormone signal, it changes in-cell cycle regulator expression and has an effect on the development of

leaves and other organs [12]. Cytokinins can increase the rate of cell division by inducing CYCD3 expression [13]. Overexpression of CYCD3;1 can replace the cytokinins required to induce callus in Arabidopsis leaves; on cytokinin-free medium, the number of tissues formed by callus was 5-times greater than the control [14]. Moreover, CYCD3;1 overexpressing Arabidopsis leaves significantly increased smaller cells and cell division replaced cell expansion as the primary mechanism for leaf growth [15].

MYC2 belongs to the bHLH gene family and is a central component of the JA signaling pathway. The MYC2 transcription factor (TF) plays a regulatory role by forming the COI1/JAZS/MYC2 complex. JAZ then binds to MYC2 and inhibits transcription at lower concentrations of JA, endogenous JA-Ile concentrations increase during environmental or developmental stimulation, the JAZ protein is degraded by the 26S proteasome, COI1 binds to JA-Ile and recruits the JAZ transcriptional repressor, and MYC2's activity is thereby restored, which then binds to the JA-reactive element (G-box) and initiates transcription [16]. Given the important role of MYC2, it has been proposed as the primary mediator of JA signaling and crosstalk along with abscisic acid, ethylene, and optical signaling pathways [17]. The myc2 mutant has a similar flowering time as wild-type Arabidopsis, while the triple mutant of myc2/3/4 exhibits an early flowering phenotype, and MYC2 is considered a negative regulator of the FT gene [18]. As the core regulator of JA, MYC2 may play an important role in multi-hormone crosstalk.

The question remains, however, as to why MYC2 and CYCD3;1 are up-regulated during flower differentiation in J. nigroviensrugosus. Is there an interaction between the two genes? The sequence cloning and expression analysis of differentially expressed genes (DEGs) are helpful for understanding the function of these genes and provide preliminary data on the underlying mechanism of flowering in J. nigroviensrugosus. This study focused on the cloning of MYC2 and CYCD3;1 gene expression and the gene expression of different tissues. Subcellular functional localization and bimolecular fluorescence complementation (BIFC) experiments were conducted in order to identify the location where JnCYCD3;1 functions and discovers complex proteins. The findings of this study will provide a basic resource for future flowering regulation and flower and fruit management.

Results

Expression correlation analysis

Results of the correlation analysis revealed that the expression of MYC2, CYCD3, and DELLA was positively correlated with different parts of J. nigroviensrugosus. CYCD3 expression was negatively correlated with JAZ (Fig. 1A). MYC2 and CYCD3 expression were positively correlated. MYC2 (gene11878) exhibited higher transcript expression levels in the inflorescence buds of cluster1 (Fig. 1B), while DELLA (gene13701) and CYCD3 (gene38) were in cluster3 and exhibited higher transcript expression levels in new leaves, followed by inflorescence buds.

Sequence structure analysis

The JnCYCD3;1 sequence was obtained by cloning, and the ORF finder predicted to obtain 534 bp. The predicted analysis revealed that the JnCYCD3;1 protein structure has a Cyclin_N conserved domain at positions 292–513. NCBI blastp alignment revealed that JnCYCD3;1 and J. curcas CYCD3 (XM_012210210.2) had 95% sequence coverage identity compared to its genomic sequence (NW_012124049.1) and XM_012210210.2. JnCYCD3;1 had an intron retention, resulting in the early termination of its coding frame (Fig. 2). The JnMYC2 sequence was also obtained by cloning. The JnMYC2 ORF was 2025 bp long, encoding 674 amino acids (aa), the protein molecular weight was 73,960.83, and the PI was 5.42. The predictive analysis revealed that JnMYC2 has a bHLH-MYC_N domain at positions 69–249, a helix-loop-helix domain at 496–547, and an SMC_N super family domain at 455–572.

Expression analysis during flowering

The quantitative expression level of fluorescence indicated that JnCYCD3;1 was expressed in all parts of the plant (Fig. 3). The highest expression levels were observed in new leaves, which were 68.42 times greater than root expression, followed by inflorescence buds; expression levels were the lowest during the pollen formation period. JnMYC2 exhibited the highest expression levels in parts of the inflorescence buds, which was 2.6 times greater than root expression. There was no difference between the expression of new leaves and female or male flowers (Fig. 4).

Subcellular function localization

The C-terminal fusion GFP expression vector, pBWA(V)HS-JnCYCD3;1-GFP, was transformed into Arabidopsis protoplasts and observed by laser confocal microscopy (Fig. 5). Green fluorescence of 35S::JnCYCD3;1 fused to GFP was observed in the nucleus. The green fluorescence was bright and coincided with the position of the nucleus Mark; thus, JnCYCD3;1 was determined to be located in the nucleus.

The C-terminal fusion GFP expression vector, pBWA(V)HS-JnMYC2-GFP, was transformed into Arabidopsis protoplasts and observed by laser confocal microscopy (Fig. 6). Green fluorescence of 35S::JnMYC2 fused with GFP was not solely present in the nucleus, showing polymerization and dispersion. JnMYC2 was distributed in both the nucleus and cytoplasm. Thus, it is speculated that JnMYC2 may possess transmembrane membrane behavior.

BIFC experiment

The transcript expression levels of MYC2, CYCD3, and DELLA were positively correlated (Fig. 1). JnMYC2 was distributed in the nucleus and cytoplasm, while JnCYCD3;1 was distributed only in the nucleus, indicating that JnMYC2 and JnCYCD3;1 could possibly interact. The results of the BIFC experiments revealed that the pairing of pBWD(LB)1C-YN(JnMYC2)-CCDB and pBWD(LA)1C-Yc(JnCYCD3;1)-CCDB exhibited fluorescence; thus, JnMYC2 and JnCYCD3;1 appear to interactively exist (Fig. 7).

Genetically modified function verification

After transgenic tobacco was differentiated and rooted (Fig. 8), it was transferred to a substrate for culturing. During the transfer process, the root medium was cleaned and placed indoors for refining. By conducting PCR (detection primers were hygromycin primers and JnCYCD3; 1 specific primers) (Table 1), transgenic tobacco was obtained for further phenotypic and functional identification.

Table 1

List of related primers.

Primer name	Primer sequence (5'-3')	Function
Actin_F	CTCCTCTCAACCCCAAAGCCAA	Reference gene
Actin_R	CACCAGAATCCAGCACGATACCA	
CYCD3-F	ACACCACAAACCCTGACCAA	Fluorescent quantitative expression
CYCD3-R	ACGAGCAACAGAGAGGGAAG	
MYC2_F	GCCTTCTTCTGGTGTGGTGA	
MYC2_R	ATTGCATCGCCAAGGAGTGA	
JnCYCD3;1_F	ATGGAACACATCAACACCACAAACC	mRNA clone
JnCYCD3;1_R	GACCCATCTCCATATCCTTCCT	
JnMYC2_F	ATGACGGACTATCGAATAGCATC	
JnMYC2_R	TCAGGTGTCACCAACTTTGGTTGAT	
pBWA(V)HS-JnCYCD3;1(+)	cagtGGTCTCacaacatggaacacatcaacaccac	Subcellular function localization
pBWA(V)HS-JnCYCD3;1(-)	cgatGGTCTCaaaagaaaaaatgacaataac	
GFP(+)	cagtGGTCTCacttttgtatcgtgaagggcgagga	
GFP(-)	cagtGGTCTCatacatcagtagagctcgtccatgc	
pBWA(V)HS-JnMYC2(+)	cagtGAAGACaacaacatgacggactatcgaatagc	
pBWA(V)HS-JnMYC2(-)	cgatGAAGACaaggtgtcaccaactttggttgat	
GFP(+)	cagtGAAGACaacacctgtatcgtgaagggcgagga	
GFP(-)	cagtGAAGACaatacatcagtagagctcgtccatgc	
JnMYC2-vn(+)	cagtGAAGACaacaagatgacggactatcgaatagc	BIFC
JnMYC2-vn(-)	cagtGAAGACaaggcgggtgtcaccaactttggttg	
JnCYCD3;1-vc(+)	cagtGGTCTCacgctatggaacacatcaacaccac	
JnCYCD3;1-vc(-)	cagtGGTCTCaaggcaaagaaaaaatgacaataac	
JnCYCD3;1(+)	ATGTTGCCGTACGATTCCGA	Transgenic molecular identification
JnCYCD3;1(-)	AAGAAAAAATGACAATAAC	
hyg(280)+	ACGGTGTCGTCCATCACAGTTTGCC	

Primer name	Primer sequence (5'-3')	Function
hyg(280)-	TTCCGGAAGTGCTTGACATTGGGGA	

Compared to wild-type tobacco, JnCYCD3;1 transgenic tobacco exhibited obvious flower formation during the seedling stage (Fig. 9). Flowers were in a fixed position, and some were formed in the stem (Fig. 9A and B), while others were formed at the top. Near the genital bud (Fig. 9C), flowers formed 5 stamen and 1 pistil (Fig. 9D–F), and the transgenic tobacco flowered considerably earlier than the wild-type plants (Fig. 9G). Subsequent observations revealed that transgenic tobacco seedlings had flowering formations at each attachment of the leaves (Fig. 9H and I), indicating that JnCYCD3;1 can considerably advance the reproductive cycle and promote flower formation and transformation.

Discussion

In previous studies, the PD-NINJA complex was found to control the initial shape of the leaf and inhibit CYCD3, thereby controlling leaf flatness in angiosperms [18]. Boucheron et al. [19] transferred CYCD3 to tobacco, which resulted in increased leaf growth rates and changes in the structure of the shoot apical meristem. Dewitte et al. [15] found that Arabidopsis leaves transfected with CYCD3 curled toward the medial axis. The A. thaliana AtCYCD3;1 gene was also found to wrinkle and curl leaves in transgenic tobacco [20]. CYCD3 overexpression caused delayed morphological differences in SAM and leaf senescence [14]. Additionally, CYCD3 was also found to be expressed at its highest levels during the flower bud stage in Rhododendron [10]. Taihangia unisexual male flowers downregulated the expression of CYCA1 and CYCD3, which resulted in the disturbance of the cell cycle in gynoecium primordia and subsequently determined the arrest of pistil development [21]. Currently, CYCD3 is the main focus of herbaceous plant investigations, which are mostly limited to overexpression. However, CYCD3 against woody plants is rarely reported, and the expression of inhibition after gene silencing is hardly described. The cyclin aa of woody plants varies widely, and existing studies have not been able to clarify the function of woody plant CYCD3. The transcription factor AINTEGUMENTA (ANT) and the D-type cyclin CYCD3;1 are expressed in the vascular cambium of Arabidopsis roots, respond to cytokinins and are both required for proper root secondary thickening, AIL1 can directly interact with the promoters of CYCD3:2 and CYCD6:1, AIL1 presumably participates in the regulation of cell division in meristematic tissues at the shoot apex [22–23]. However, there are few reports on the regulation of flowering by CYCD3 in woody plants, and the expression of inhibition after gene silencing is hardly recorded, and the expression of inhibition after gene silencing is hardly described. The cyclin aa of woody plants varies widely, and existing studies have not been able to clarify the function of woody plant CYCD3.

Typical animal or plant cyclins contain a conserved region called the cyclin core, which is ~ 250 aa and consists of 2 domains: Cyclin_N and Cyclin_C. Cyclins have certain structural differences, but they all have highly conserved cyclin cassette sequences. Cyclin_N is required for the binding and activation of cyclin-dependent kinase (CDK), while Cyclin_C is less conserved and may not be present in some cyclins [24–27]. Arabidopsis C-, D-, H-, T-, L-, and P-type cyclins have a Cyclin_N domain, but no Cyclin_C domain;

thus, the Cyclin_C domain may not be critical for its function [28]. Intron retention is the most common alternative splicing form in plants [29]. In JnCYCD3;1, retention of the first intron leads to its coding frame in advance. However, the termination or loss of the Cyclin_C domain, whose structural differences may lead to changes in traits, requires further investigation. The expression pattern of CYCD3 in different tissues of 2 varieties of J. curcas was essentially the same, and both were the highest expressed in young leaves, followed by inflorescence buds during the differentiation process. Transcript abundance of CYCD3;1 increased more than 5-fold during the early stages of L1 flower development (the first 10 inflorescences of each tomato plant retaining the fruit of the second inflorescence) and is possibly involved in cell cycle regulation in response to mitosis signals [30]. Brassica napus BnCYCD3-1-like-2-1 and BnCYCD3-1-like-2-2 are different splicing bodies of the same gene and have the highest expression levels in leaves. Additionally, the variable cleavage of CYCD3:1 could possibly help rapeseed cope with environmental stress by coordinating the transcript levels of different splices [31].

Subcellular functional localization indicated that JnCYCD3;1 functions in the nucleus. BIFC experiments indicated that JnMYC2 interacts with JnCYCD3;1. The transgenic seedlings demonstrated that JnCYCD3;1 can considerably advance the reproductive cycle, which may promote flower formation and transformation. However, the cause of this phenomenon, as well as research on transcription, metabolism, and late phenotypes of wild-type plants, requires further investigation. Because tobacco is a hermaphroditic plant, if JnCYCD3;1 leads to the proliferation of female flower primordia, it is necessary to construct a related overexpression/RNAi vector and introduce it to medicinal J. curcas/nigroviensrugosus in future observations.

Conclusion

In this study, comparative transcriptomics data, using ene cloning, relative fluorescence quantification, and subcellular functional localization, were used to explore the reproductive advantages of J. nigroviensrugosus. The JnCYCD3;1 ORF was found to be 414 bp, encoding 137 aa. Compared to J. curcas, the presence of intron retention led to early termination of the coding frame. RT-qPCR indicated that JnCYCD3;1 exhibited the highest expression levels in new leaves, which was 68.42 times greater than root expression, followed by inflorescence buds. JnCYCD3;1 was also found to play a role in the nucleus. BIFC experiments demonstrated that JnMYC2 interacts with JnCYCD3;1. JnCYCD3; 1 transgenic tobacco considerably advanced the reproductive cycle and may promote flowering formation and transformation.

Methods

Materials

Experimental materials were obtained from 8-year-old J. nigroviensrugosus found in the Qiaoma Forest Farm, Ceheng County, Guizhou Province, China. None permissions were necessary to collect such samples, the specie was confirmed to be J. nigroviensrugosus by the Professor Xu Gang and Fan Fuhua

(Institute for Forest Resources & Environment of Guizhou, Guizhou University), the voucher specimen is accessible at the Institute for Forest Resources & Environment of Guizhou, Guizhou University (accessions No. JN-001-1). This plant is not an endangered plant. Related experimental research, including the collection of plant materials, complies with institutional, national or international guidelines. Mature leaves of J. nigroviensrugosus were used as cloning materials. Fluorescent quantitative materials were collected as follows: (1) Jn_r: roots (main roots); (2) Jn_s:stems; (3) Jn_l: young leaves (red-red neonatal leaf buds at the top of shoots) during the flowering stage; (4) Jn_p: inflorescence bud formation stage (buds at the top of the branches of sex differentiation forming protrusions at the inflorescence axis, diameter < 0.3 cm); (5) Jn_fd: floret differentiation stage (apical flower bud differentiation forming the third main inflorescence); (6) Jn_m: unopened male flowers (bracts and petals of male flowers had not unfolded, yellow anthers were slightly visible to the naked eye after a longitudinal cut); (7) Jn_f: unopened female flowers (bracts and petals of female flowers had not unfolded, white ovules were slightly visible to the naked eye after slitting); (8) Jn_pp: female flower ovary developmental stage (female flower apex differentiates from stigma 2–4 and the top splits); and (9) Jn_pf: male flower pollen formation period (male flower bracts and petals bend outward, confluent filament formed a hollow channel, anther was separated).

Each sample had 3 biological replicates. Samples were wrapped in foil and quickly placed in liquid nitrogen, then kept in an ultra-low temperature freezer at -80 °C for future analyses. Subcellular functional localization experimental materials were obtained from Arabidopsis protoplasts. Nicotiana benthamiana was used as transgenic material.

Experimental methods

Correlation analysis of transcript expression

Focusing on the differential gene set in the plant hormone signaling pathway of the buds of 2 varieties, expression correlations and trends in different parts of the plant were analyzed [8]. A correlation circle map was created using the R circlize package [32]. The clustering of expression trends was performed using Python DP_GP [33].

RNA extraction and cDNA synthesis

Extraction of total RNA from the samples was conducted using an EASYSPIN plus plant RNA extraction kit following the manufacturer's instructions. After RNA extraction, the quality was verified. First-strand synthesis of the cDNA was conducted using an EasyScript First-Strand cDNA Synthesis SuperMix kit following the manufacturer's instructions.

Cloning the gene of interest

Specific primers were designed using the J. curcas genome (Table 1). The PCR reaction system consisted of 10.5 μL ddH_2O, 12.5 μL PCR mix, 1.0 μL cDNA template, and 1.0 μL of upstream and downstream primers each (25.0 μL total). The PCR product was observed by gel electrophoresis. The product was

recovered, ligated into the PGEM-T vector, transformed into E. coli competent cells, and subjected to blue-white screening and colony PCR verification. Positive clones were sent for sequencing.

RT-qPCR verification

Real-time (RT)-quantitative (q) PCR amplification was conducted using an SYBR Premix Ex TaqTM II kit. The reaction system consisted of 10.0 μL 2 × SYBR Premix Ex TaqTM II kit mix, 0.8 μL qRT-F and qRT-R each, 1.0 μL cDNA, and 7.4 μL ddH_2O (20.0 μL total). The amplification procedure was as follows: pre-denaturation at 95 °C for 30 s; 40 cycles at 95 °C for 15 s, 58 °C for 15 s, and 72 °C for 15 s. Each sample was repeated 3 times. The actin gene was used as the reference gene [34].

Subcellular functional localization and BIFC experiments

According to JnCYCD3;1, due to JnMYC2's gene sequence and vector characteristics, the pBWA(V)HS-ccdb-GLosgfp vector was selected. The vector was constructed by the golden gate technique [35]. The vector was ligated, and 5–10 μL of the ligation product was transformed into Escherichia coli. The plate was transformed with a transformant (carnamycin) resistant plate and cultured at 37 °C for 12 h for plaque PCR identification. The correct plasmid was preserved by sequencing. The constructed vector plasmid was transferred into Agrobacterium, and the cells were suspended, collected, resuspended, and transformed into Arabidopsis protoplasts. According to the preliminary positioning result, Mark was selected for co-localization.

GM functional verification

Mature tobacco embryos were used to induce sterile tobacco seedlings, and the Agrobacterium suspension was subsequently prepared. Tobacco leaves were cut into ~ 5 × 5 mm pieces and placed in Agrobacterium suspension (0D600 = ~ 0.4–0.6) for full contact and infection. After gently shaking for 8 min, surface bacterial liquid was washed with sterilized water. Leaves were placed face up on tobacco differentiation medium and cultured in a dark incubator at 28 °C for 2 d. Co-cultured leaves were transferred to pre-screening medium for subsequent screening. After ~ 7 d of recovery, leaves on the pre-screen were transferred to differentiation medium supplemented with antibiotics. After seedlings had grown, they were cut and inoculated into new rooting medium for ~ 10 d for subsequent molecular identification. Plant DNA was extracted, and the JnCYCD3;1 gene-specific primer was used to amplify and detect whether tobacco seedling contained the gene by conventional PCR.

Abbreviations

aa
amino acid
BIFC
bimolecular fluorescence complementation
cDNA
Complementary DNA

DEGs
differentially expressed genes
KNAT6
knotted1-like homeobox gene 6
J. nigroviensrugosus
K. Jatropha nigroviensrugosus
J. curcas
Jatropha curcas
ORF
open reading frame
RT-qPCR
Real-time (RT)-quantitative (q) PCR

Declarations

Ethics approval and consent to participate

Not applicable.

Consent for publication

Not applicable.

Availability of data and materials

Amplification curves and melting peaks of RT-qPCR can be found in the Additional file 1; The negative control of BIFC experiment can be found in the Additional file 2. The datasets used and analyzed during the current study could be available from the corresponding author on request.

Competing interests

The authors declare that they have no competing interests.

Funding

The work was supported by National Natural Science Foundation of China-Study on flower bud differentiation and flowering mechanism of *Jatropha nigroviensrugosus* CV Yang. (31360165). The funding body was not involved in the design of the study, analysis, and interpretation of data in the manuscript.

Authors' contributions

X.F and Z.Y designed and executed the experiment; W.X.R conductedadditional analyses; X.F wrote the manuscript. All authors have read and approved the manuscript.

Acknowledgments

Not applicable.

References

1. Yang C Y, Fang Z, Li B, et al. Review and prospects of *Jatropha* biodiesel industry in China. Renewable and Sustainable Energy Reviews, 2012;16(4): 2178-2190.
2. Yang, C, Lu, W, Wu, X, Xu, Z, & Long, Y. Analysis on Components of Fatty Acids from New *Jatropha* Cultivars Seed Oils and Their Potential of Preparing Biodiesel. Botanical Research, 2015;4(1), 16-24.
3. Gangwar M, Sood H, Chauhan R S, Genomics and relative expression analysis identifies key genes associated with high female to male flower ratio in *Jatropha curcas* Molecular biology reports, 2016;43(4): 305-322.
4. Xu, G, Huang, J, Yang, Y, & Yao, Y. A. Transcriptome analysis of flower sex differentiation in *Jatropha curcas* using RNA sequencing. PloS one, 2016;11(2), e0145613.
5. Hui W, Yang Y, Wu G, et al. Transcriptome profile analysis reveals the regulation mechanism of floral sex differentiation in *Jatropha curcas* Scientific reports, 2017;7(1): 16421.
6. Chen M S, Pan B Z, Wang G J, et al. Analysis of the transcriptional responses in inflorescence buds of *Jatropha curcas* exposed to cytokinin treatment. BMC plant biology, 2014;14(1): 318.
7. Gangwar M, Sood A, Bansal A, et al. Comparative transcriptomics reveals a reduction in carbon capture and flux between source and sink in cytokinin-treated inflorescences of *Jatropha curcas* 3 Biotech, 2018;8(1): 64.
8. Xiao F, Wang X R, Zhao Y, et al. Flowering Related Comparative Transcriptomics between *Jatropha curcas* and *Jatropha nigroviensrugosus*. INTERNATIONAL JOURNAL OF AGRICULTURE AND BIOLOGY, 2018;20(7): 1523-1532.
9. Chen M S, Pan B Z, Fu Q, et al. Comparative transcriptome analysis between gynoecious and monoecious plants identifies regulatory networks controlling sex determination in *Jatropha curcas*. Frontiers in plant science, 2017;7: 1953.
10. Wang S, Li Z, Jin W, et al. Transcriptome analysis and identification of genes associated with flower development in *Rhododendron pulchrum* Sweet (Ericaceae). Gene, 2018;679: 108-118.
11. Pan B Z, Chen M S, Ni J, et al. Transcriptome of the inflorescence meristems of the biofuel plant *Jatropha curcas* treated with cytokinin. BMC genomics, 2014;15(1): 974.
12. de Jager S M, Maughan S, Dewitte W, et al. The developmental context of cell-cycle control in plants//Seminars in cell & developmental biology. Academic Press, 2005;16(3): 385-396.
13. D'Agostino I B, Kieber J J, Molecular mechanisms of cytokinin action. Current opinion in plant biology, 1999;2(5): 359-364.
14. Riou-Khamlichi C, Huntley R, Jacqmard A, et al. Cytokinin activation of *Arabidopsis* cell division through a D-type cyclin. Science, 1999; 283(5407): 1541-1544.

15. Dewitte W, Riou-Khamlichi C, Scofield S, et al. Altered cell cycle distribution, hyperplasia, and inhibited differentiation in *Arabidopsis* caused by the D-type cyclin CYCD3. The Plant Cell, 2003; 15(1): 79-92.
16. Cui M, Du J, Yao X J. The binding mechanism between inositol phosphate (InsP) and the jasmonate receptor complex: a computational study. Frontiers in plant science, 2018; 9: 963.
17. Hong G J, Xue X Y, Mao Y B, et al. *Arabidopsis* MYC2 interacts with DELLA proteins in regulating sesquiterpene synthase gene expression. The Plant Cell, 2012; 24(6): 2635-2648.
18. Baekelandt A, Pauwels L, Wang Z, et al. *Arabidopsis* leaf flatness is regulated by PPD2 and NINJA through repression of CYCLIN D3 genes. Plant physiology, 2018; 178(1): 217-232.
19. Boucheron E, Healy J H S, Bajon C, et al. Ectopic expression of *Arabidopsis* CYCD2 and CYCD3 in tobacco has distinct effects on the structural organization of the shoot apical meristem. Journal of experimental botany, 2004; 56(409): 123-134.
20. Lijuan D, Tangchun Z, Caixia L, et al. Construction of plant expression vector and genetic transformation analysis of *Arabidopsis thaliana* CYCD3;1 gene in Nicotiana tabacum. Journal of Anhui Agricultural University, 2016; 43 (06): 996-1003
21. Li W, Zhang L, Ding Z, et al. De novo sequencing and comparative transcriptome analysis of the male and hermaphroditic flowers provide insights into the regulation of flower formation in andromonoecious Taihangia rupestris. BMC plant biology, 2017; 17(1): 54.
22. Randall R S, Miyashima S, Blomster T, et al. AINTEGUMENTA and the D-type cyclin CYCD3; 1 regulate root secondary growth and respond to cytokinins. Biology open, 2015; 4(10): 1229-1236.
23. Maurya J P, Bhalerao R P. Photoperiod-and temperature-mediated control of growth cessation and dormancy in trees: a molecular perspective. Annals of botany, 2017; 120(3): 351-360.
24. Nugent J H, Alfa C E, Young T, et al. Conserved structural motifs in cyclins identified by sequence analysis. Journal of cell science, 1991; 99(3): 669-674.
25. Horne M C, Goolsby G L, Donaldson K L, et al. Cyclin G1 and cyclin G2 comprise a new family of cyclins with contrasting tissue-specific and cell cycle-regulated expression. Journal of Biological Chemistry, 1996; 271(11): 6050-6061.
26. Murray A W. Recycling the cell cycle: cyclins revisited. Cell, 2004; 116(2): 221-234.
27. Wang G, Kong H, Sun Y, et al. Genome-wide analysis of the cyclin family in Arabidopsis and comparative phylogenetic analysis of plant cyclin-like proteins. Plant physiology, 2004;135(2): 1084-1099.
28. Ma Z, Wu Y, Jin J, et al. Phylogenetic analysis reveals the evolution and diversification of cyclins in eukaryotes. Molecular phylogenetics and evolution, 2013; 66(3): 1002-1010.
29. Ullah F, Hamilton M, Reddy A S N, et al. Exploring the relationship between intron retention and chromatin accessibility in plants. BMC genomics, 2018; 19(1): 21.
30. Baldet P, Hernould M, Laporte F, et al. The expression of cell proliferation-related genes in early developing flowers is affected by a fruit load reduction in tomato plants. Journal of Experimental Botany, 2006; 57(4): 961-970.

31. Guo Y, Li J, Fang Y, et al. An event of alternative splicing affects the expression of two BnCYCD3-1-like genes in Brassica napus. Gene, 2019; 694: 33-41.
32. Gu Z, Gu L, Eils R, et al. circlize implements and enhances circular visualization in R. Bioinformatics, 2014; 30(19): 2811-2812.
33. McDowell I C, Manandhar D, Vockley C M, et al. Clustering gene expression time series data using an infinite Gaussian process mixture model. PLoS computational biology, 2018; 14(1): e1005896.
34. Zhang L, He L L, Fu Q T, et al. Selection of reliable reference genes for gene expression studies in the biofuel plant *Jatropha curcas* using real-time quantitative PCR. International journal of molecular sciences, 2013; 14(12): 24338-24354.
35. Engler C, Gruetzner R, Kandzia R, et al. Golden gate shuffling: a one-pot DNA shuffling method based on type IIs restriction enzymes. PloS one, 2009; 4(5): e5553.

Figures

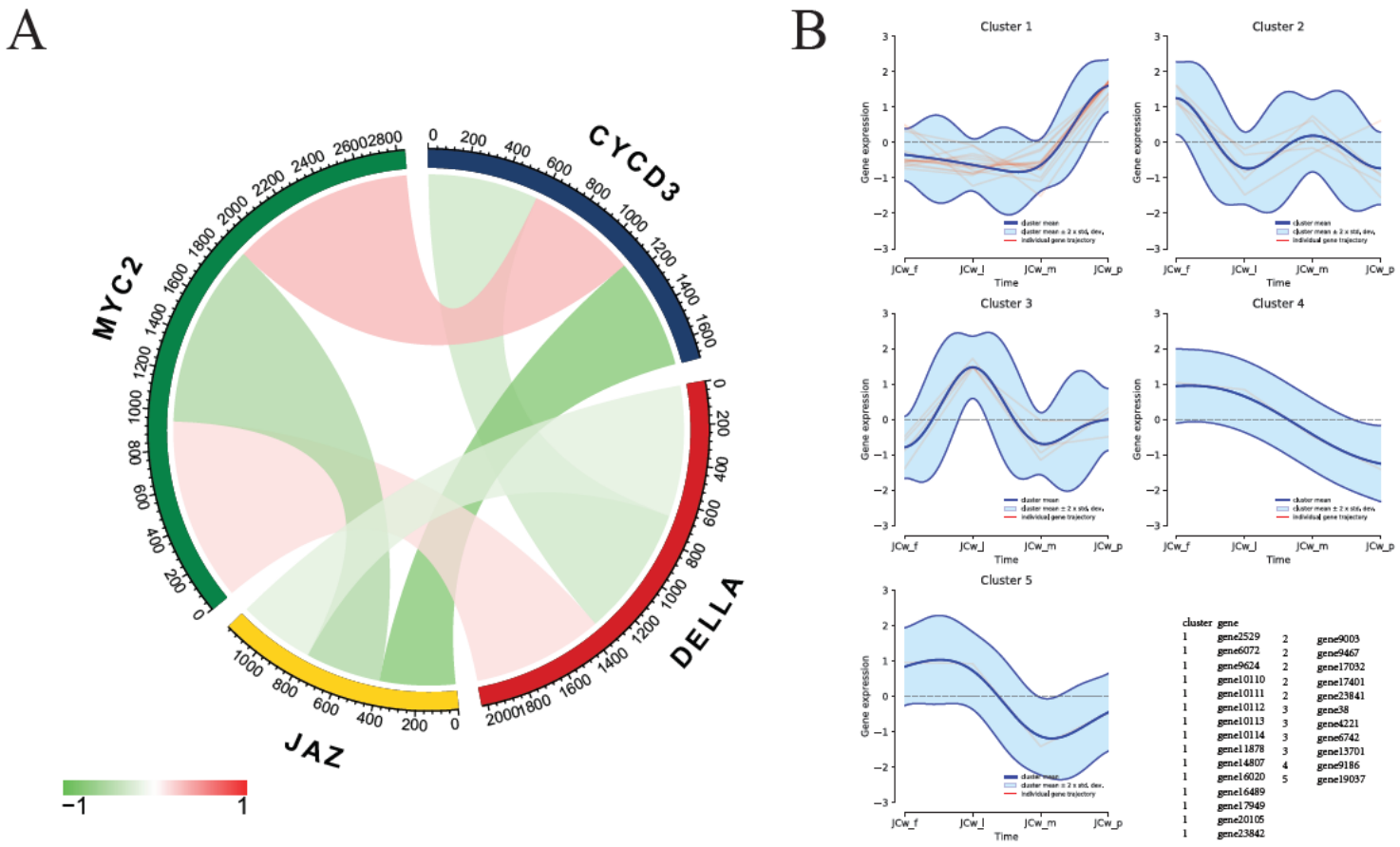

Figure 1

Correlation and trend expression of differentially expressed genes. A: Gene expression correlation diagram; B: Gene expression trend diagram. Note: A: red represents positive correlation, green represents negative correlation, the deeper the color, the greater the correlation coefficient; B:Trends of expression of

hormone-related differentially expressed genes in inflorescence bud (sex differentiation term) between of J. curcas and J. nigroviensrugosus; JCw_f: unopened female flower; JCw_l: new born young leaves; JCw_m: unopened male flower; JCw_p: Inflorescence bud

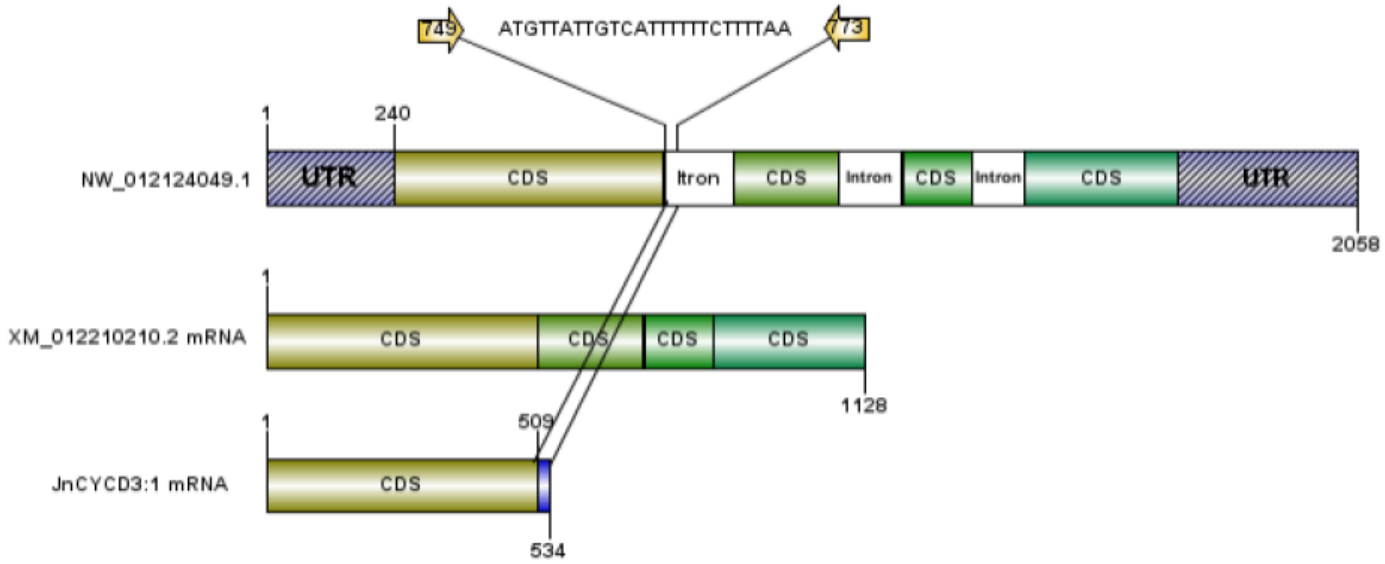

Figure 2

Schematic diagram of JnCYCD3;1.

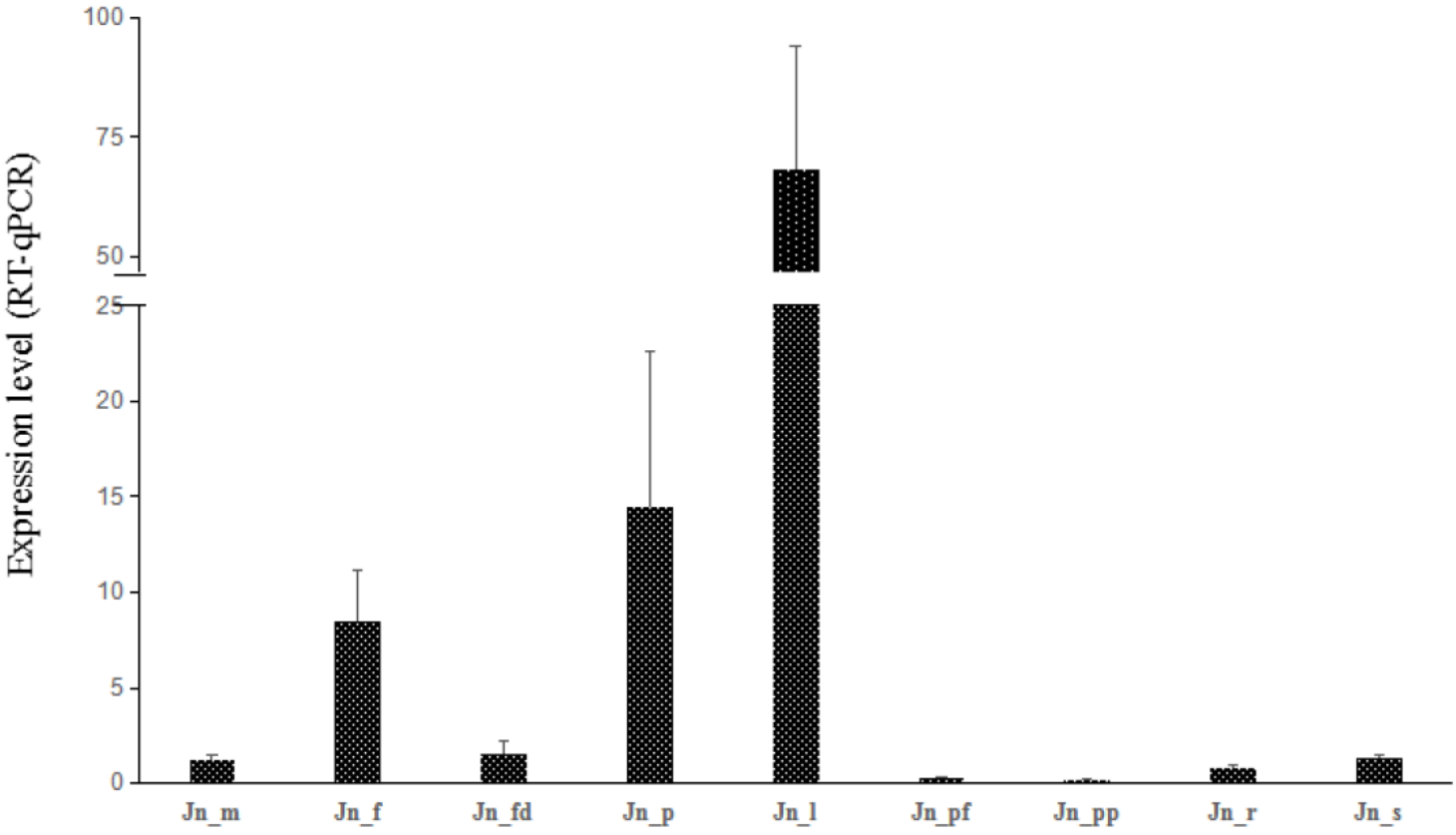

Figure 3

Expression level of JnCYCD3 in different tissue sites of J. nigroviensrugosus. Jn_m: unopened male flower; Jn_f: unopened female flower; Jn_fd: florescence differentiation period; Jn_p: inflorescence bud; Jn_l: new born young leaves; Jn_pf: male flower pollen formation period; Jn_pp: female flower ovary developmental stage; Jn_r: main root; Jn_s: stem formation layer. Error bars represent the standard deviation (SD).

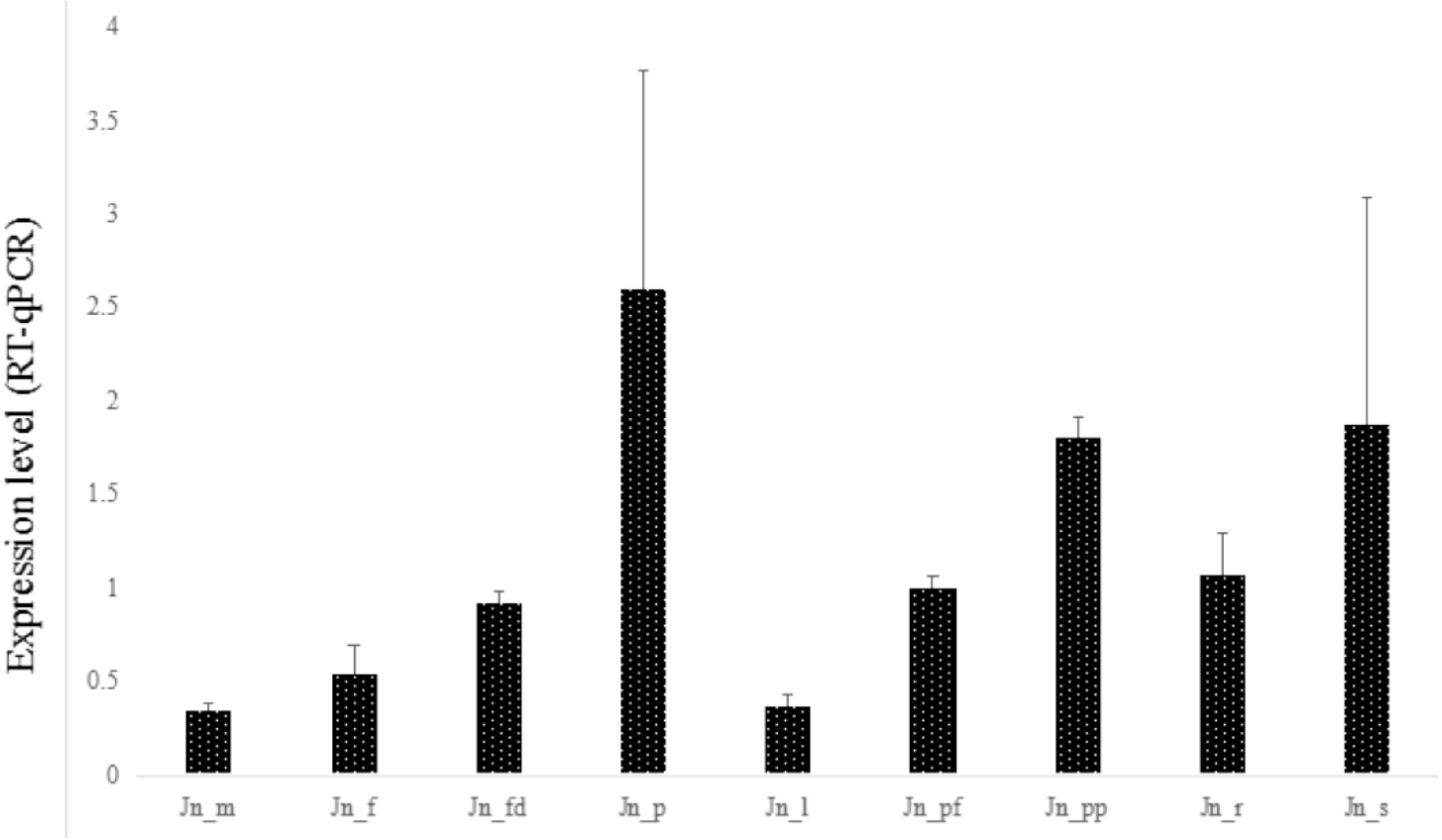

Figure 4

Expression level of JnMYC2 in different tissue sites of J. nigroviensrugosus. Jn_m: unopened male flower; Jn_f: unopened female flower; Jn_fd: florescence differentiation period; Jn_p: inflorescence bud; Jn_l: new born young leaves; Jn_pf: male flower pollen formation period; Jn_pp: female flower ovary developmental stage; Jn_r: main root; Jn_s: stem formation layer. Error bars represent the SD.

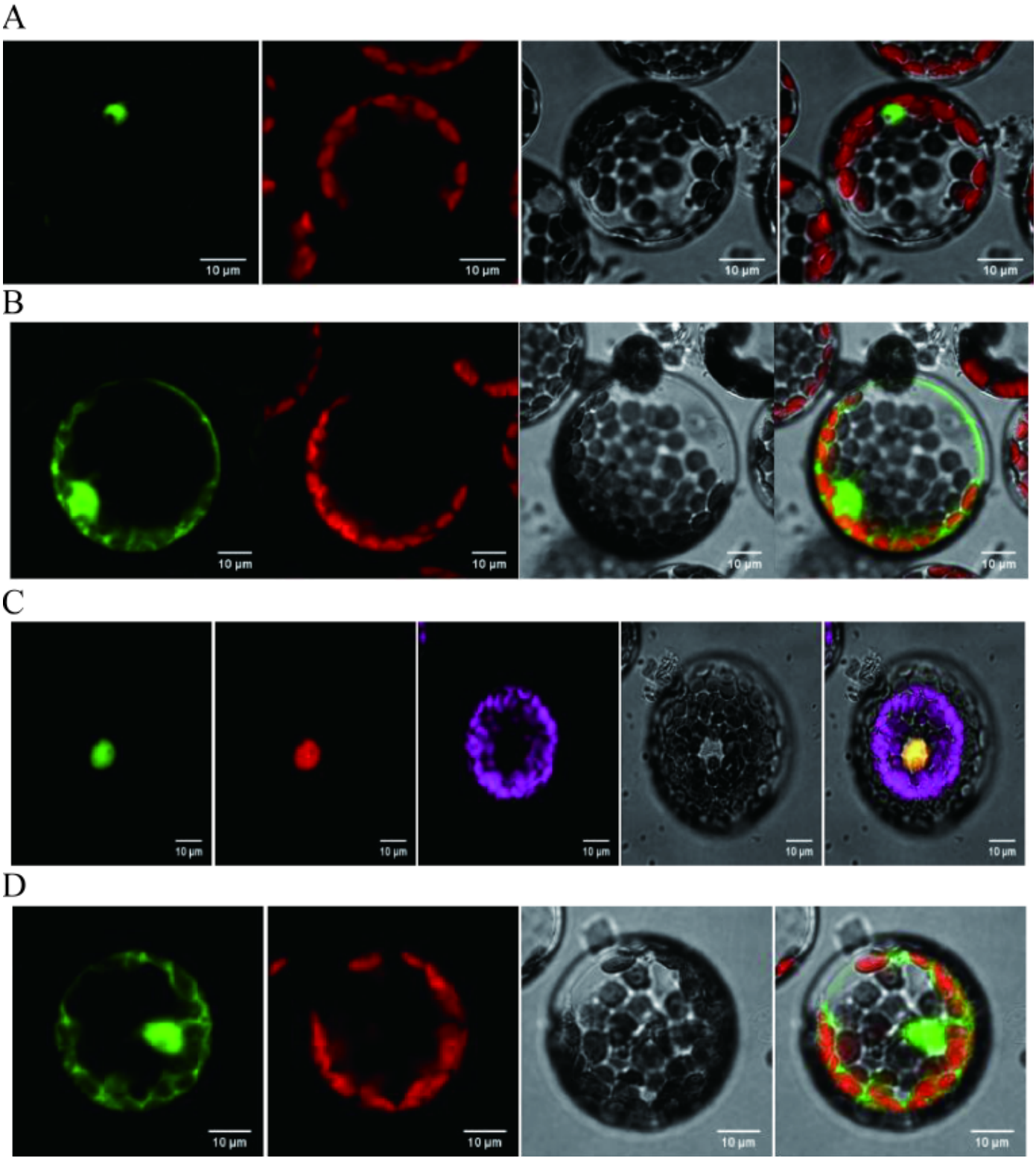

Figure 5

Subcellular localization results of JnCYCD3;1 in Arabidopsis protoplasts. A: The target protein fluorescence channel, chloroplast channel, bright field, and superimposed map (from left to right); B: Empty vector control of the fluorescence channel, chloroplast channel, bright field, and superimposed map (from left to right); C The target protein fluorescence channel, marker fluorescence channel,

chloroplast channel, bright field, and superimposed map (from left to right); D: The empty vector control of the fluorescence channel, chloroplast channel, bright field, and superimposed map (from left to right).

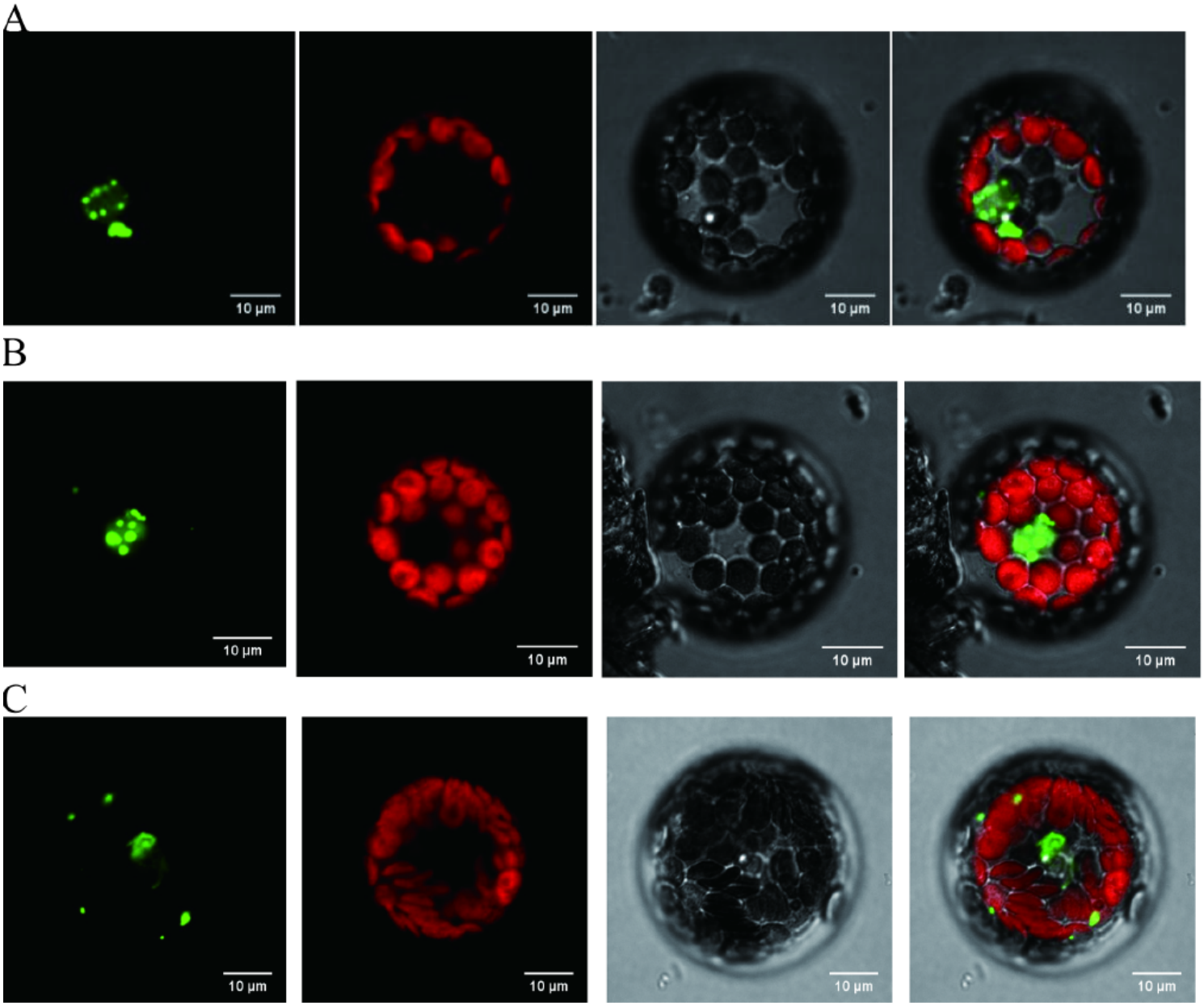

Figure 6

Subcellular localization results of JnMYC2 in Arabidopsis protoplasts. A–C: The target protein fluorescence channel, chloroplast channel, bright field, and superimposed map (from left to right); D: Empty vector control of the fluorescence channel, chloroplast channel, bright field, and superimposed map (from left to right)

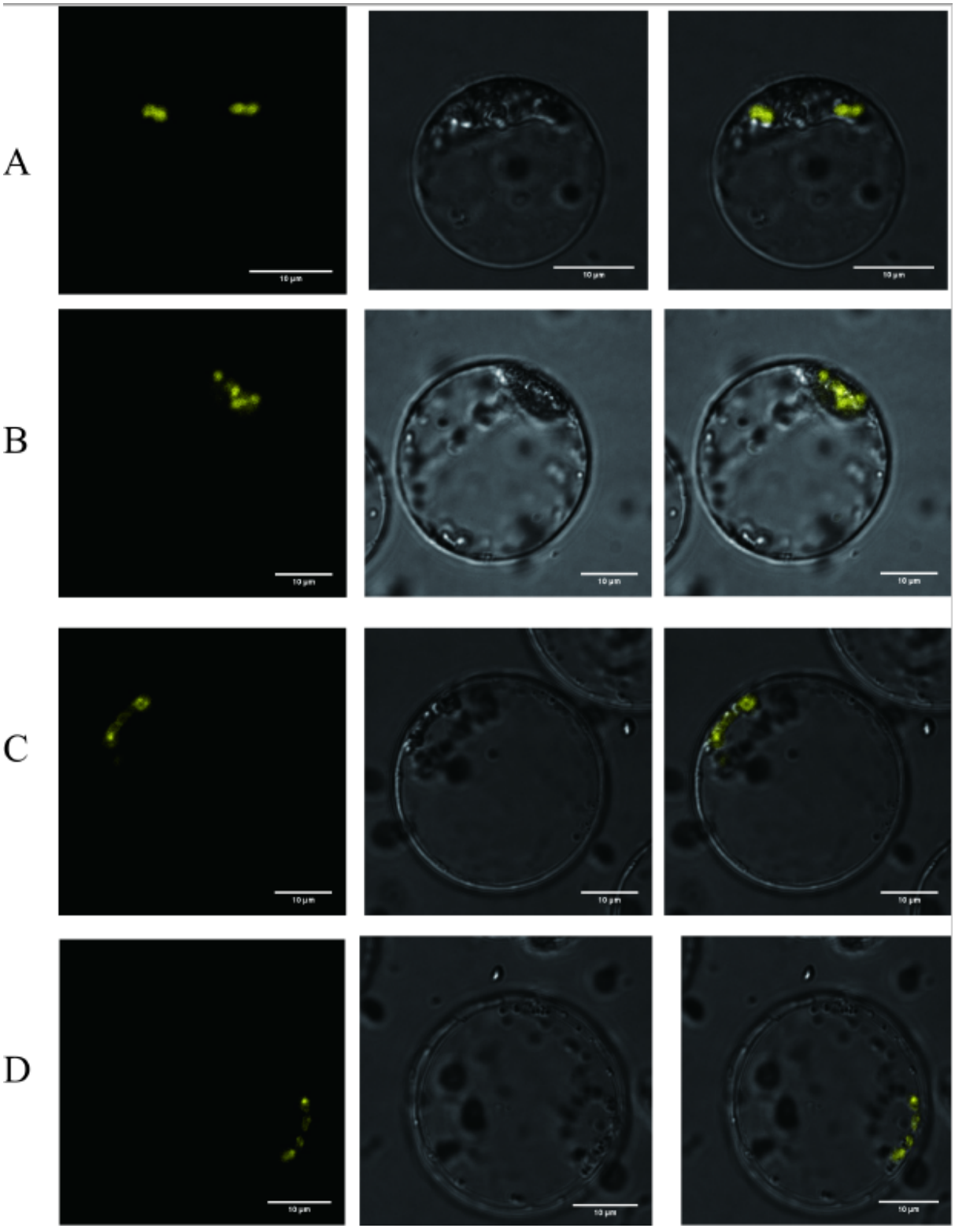

Figure 7

JnMYC2 and JnCYCD3;1 BIFC experiments. A–D: the target protein fluorescence channel, bright field, and overlay (from left to right).

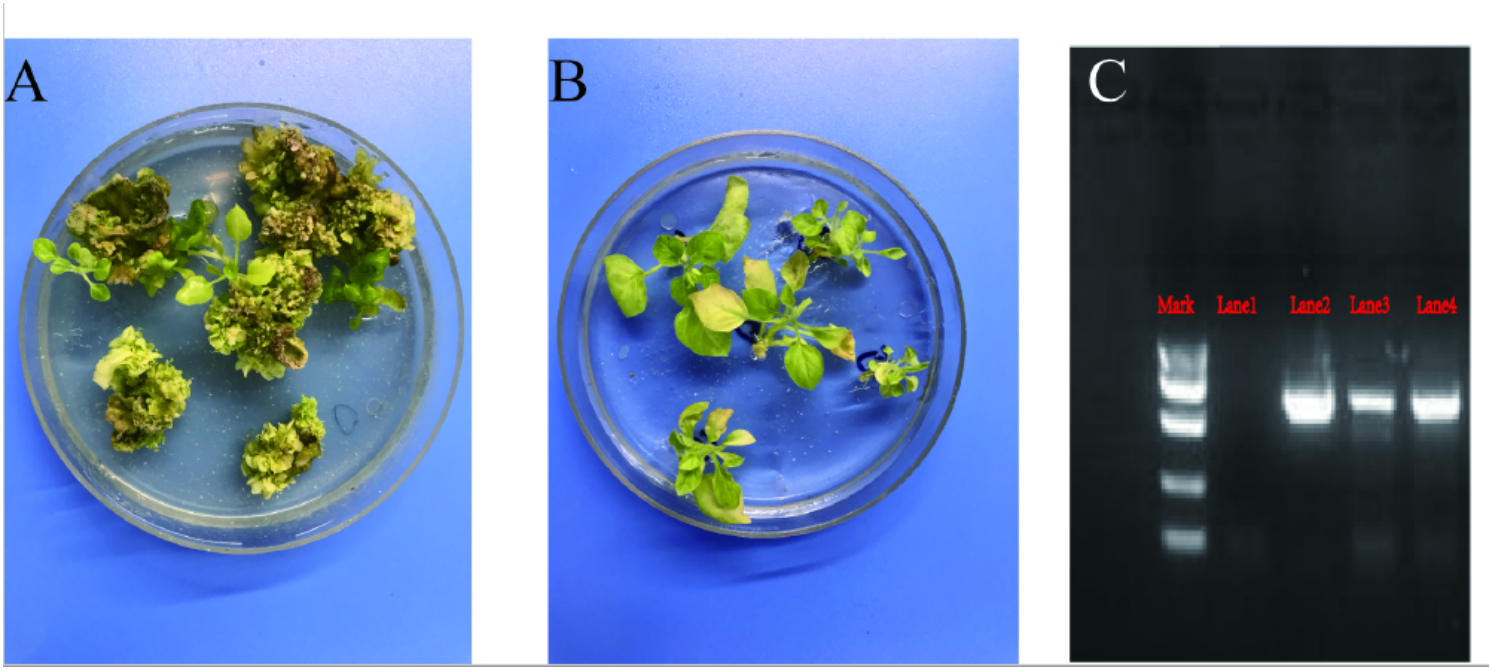

Figure 8

Identification of genetically modified tobacco. A: Transgenic JnCYCD3;1 tobacco differentiation stage; B: transgenic JnCYCD3;1 tobacco rooting stage; C: Identification of transgenic molecules (note: lane1 is the negative control; lane2 is the positive plasmid control; lanes 3 and 4 are transgenic vaccine samples).

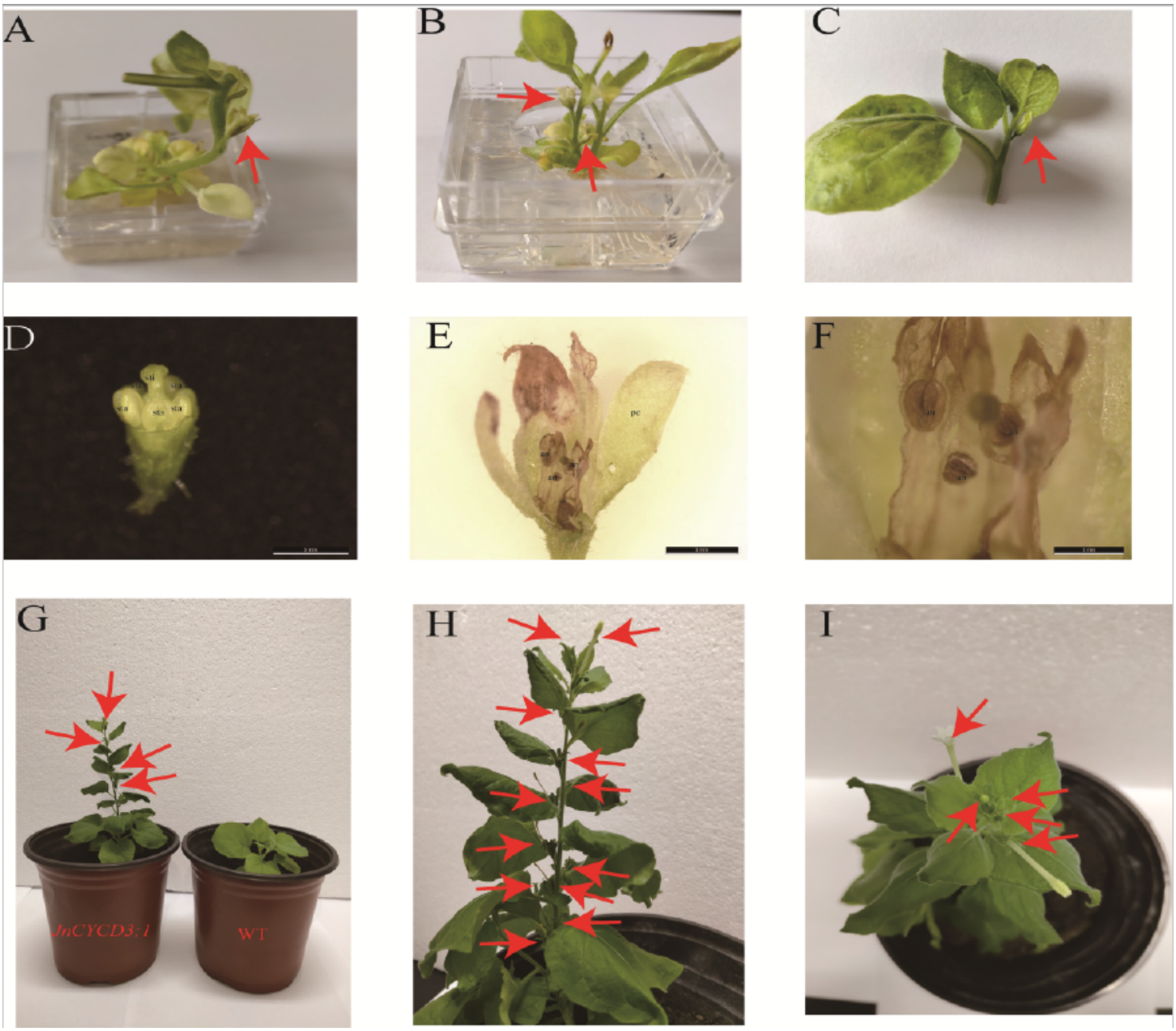

Figure 9

Phenotype of genetically modified tobacco. A–C: JnCYCD3;1 transgenic tobacco seedling phenotype (red arrow indicates the location of the flower organ); D–F: floral organ structure; G: 30 d JnCYCD3;1 transgenic tobacco seedlings and wild-type tobacco (control); H: main of view of 60 d JnCYCD3;1 transgenic tobacco; I: top view of 60 d JnCYCD3;1 transgenic (note: stamen, stigma (sti), anther (an), petal (pe)).

Supplementary Files

This is a list of supplementary files associated with this preprint. Click to download.

- Supplementaryfile2.pdf
- Supplementaryfile1.pdf